

## Raman Scattering in Alloy Semiconductors: "Spatial Correlation" Model

P. Parayanthal and Fred H. Pollak

*Department of Physics, Brooklyn College of the City University of New York, Brooklyn, New York 11210*

(Received 8 November 1983)

Using a "spatial correlation" model with a Gaussian correlation function we have for the first time quantitatively explained the broadening and asymmetry of the first-order longitudinal-optic phonon Raman spectrum induced by alloy potential fluctuations. The systems studied were the representative alloy semiconductors  $\text{Ga}_{1-x}\text{Al}_x\text{As}/\text{GaAs}$  and  $\text{Ga}_{0.47}\text{In}_{0.53}\text{As}/\text{InP}$ . This analysis provides important insights into the microscopic nature of the alloy potential fluctuations.

PACS numbers: 63.20.-e, 61.55.Hg, 63.50.+x

One of the most important aspects of substitutional semiconductor alloys is the nature of the alloy potential fluctuations (APF). Since Raman scattering can yield important information about the nature of the solid on a scale of the order of a few lattice constants, it can be used to study the microscopic nature of structural and/or topological disorder. Although there has been a number of Raman studies of alloy semiconductors,<sup>1,2</sup> only recently has the relation between alloy disorder and the line shape (i.e., linewidth and asymmetry) of allowed modes been noted.<sup>3,4</sup>

In this Letter we present a model which for the first time quantitatively accounts for the details of the first-order Raman line shape (broadening and broadening asymmetry) induced by the APF in alloy semiconductors.<sup>5</sup> We have analyzed the longitudinal-optic (LO) phonon line shape in the representative alloy semiconductors  $\text{Ga}_{1-x}\text{Al}_x\text{As}/\text{GaAs}$  (two-mode behavior) and  $\text{Ga}_{0.47}\text{In}_{0.53}\text{As}/\text{InP}$  (apparent one-mode behavior) using a "spatial correlation" model, based on finite phonon mode correlations related to  $q$ -vector relaxation induced by the microscopic nature of the alloy disorder. The APF destroy translational invariance, an effect that manifests itself as a breakdown of the usual  $\vec{q}=0$  Raman selection rule, thus leading to broadening and asymmetry of the Raman line shape. Our interpretation makes it possible to use Raman spectra to evaluate an average "spatial correlation length" and hence to obtain valuable insights into the microscopic nature of the alloy disorder. The relation of our work to Ref. 3 will be discussed.

Raman spectra were obtained on a number of samples of  $\langle 100 \rangle$   $\text{Ga}_{1-x}\text{Al}_x\text{As}/\text{GaAs}$  ( $0 \leq x \leq 0.9$ ) and  $\langle 100 \rangle$   $\text{Ga}_{0.47}\text{In}_{0.53}\text{As}/\text{InP}$  prepared by a variety of growth techniques. Characteristics of the samples are listed in Table I. Measurements were

made at 300 K in the backscattering geometry, using the 5145-Å line of an  $\text{Ar}^+$  laser. The composition  $x$  in  $\text{Ga}_{1-x}\text{Al}_x\text{As}$  was determined from the frequency positions of the LO phonon peaks.<sup>6,7</sup>

Figure 1 shows the Raman spectra from GaAs ( $x=0$ ) as well as three samples of  $\text{Ga}_{1-x}\text{Al}_x\text{As}/\text{GaAs}$  ( $x=0.3, 0.5, \text{ and } 0.9$ ). In the backscattering geometry from  $\langle 100 \rangle$  only the LO phonon modes were allowed and hence we will concentrate on these structures. The GaAs spectrum shows a symmetric ( $\Gamma_a = \Gamma_b$ ), Lorentzian line shape with a natural linewidth  $\Gamma_0 (= \Gamma_a + \Gamma_b)$  of  $3.0 \text{ cm}^{-1}$  (corrected for instrumental resolution).  $\text{Ga}_{1-x}\text{Al}_x\text{As}$  ex-

TABLE I. Characteristics of the  $\text{Ga}_{1-x}\text{Al}_x\text{As}/\text{GaAs}$  and  $\text{Ga}_{0.47}\text{In}_{0.53}\text{As}/\text{InP}$  samples in Fig. 3. The notation for growth techniques is as follows: MOCVD, metal-organic chemical vapor deposition; MBE, molecular-beam epitaxy; LPE, liquid-phase epitaxy; VPE, vapor-phase epitaxy.

Sample	Material	Growth technique
1	$\text{Ga}_{0.79}\text{Al}_{0.21}\text{As}/\text{GaAs}$	MOCVD
2	$\text{Ga}_{0.7}\text{Al}_{0.3}\text{As}/\text{GaAs}$	MBE
3	$\text{Ga}_{0.64}\text{Al}_{0.36}\text{As}/\text{GaAs}$	MBE
4	$\text{Ga}_{0.6}\text{Al}_{0.4}\text{As}/\text{GaAs}$	MBE
5	$\text{Ga}_{0.6}\text{Al}_{0.4}\text{As}/\text{GaAs}$	Ref. 3
6	$\text{Ga}_{0.5}\text{Al}_{0.5}\text{As}/\text{GaAs}$	LPE
7	$\text{Ga}_{0.18}\text{Al}_{0.82}\text{As}/\text{GaAs}$	LPE
8	$\text{Ga}_{0.1}\text{Al}_{0.9}\text{As}/\text{GaAs}$	LPE
9	$\text{Ga}_{0.1}\text{Al}_{0.9}\text{As}/\text{GaAs}$	LPE
10	$\text{Ga}_{0.47}\text{In}_{0.53}\text{As}/\text{InP}$	MOCVD
11	$\text{Ga}_{0.47}\text{In}_{0.53}\text{As}/\text{InP}$	LPE
12	$\text{Ga}_{0.47}\text{In}_{0.53}\text{As}/\text{InP}$	MOCVD
13	$\text{Ga}_{0.47}\text{In}_{0.53}\text{As}/\text{InP}$	MBE
14	$\text{Ga}_{0.47}\text{In}_{0.53}\text{As}/\text{InP}$	MBE
15	$\text{Ga}_{0.47}\text{In}_{0.53}\text{As}/\text{InP}$	VPE

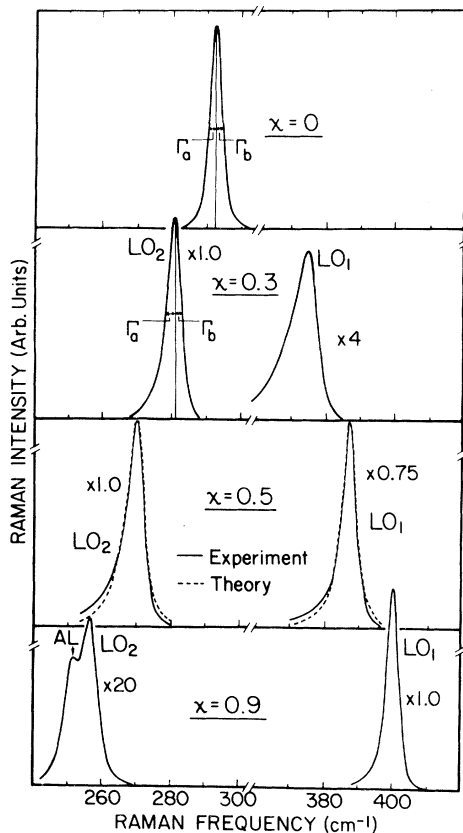


FIG. 1. Raman spectra from the  $\langle 100 \rangle$  surface of  $\text{Ga}_{1-x}\text{Al}_x\text{As}/\text{GaAs}$  at 300 K for  $x=0.0, 0.3, 0.5,$  and  $0.9$ . A small background due to the disorder-activated TO phonons has been subtracted from the low-energy side of the alloy spectra. The dashed lines show the fit obtained from the theoretical model [Eqs. (1) and (2) using correlation lengths 62 and 80 Å for  $\text{LO}_2$  and  $\text{LO}_1$ , respectively].

hibits a two-mode behavior, i.e., an “AlAs-like” mode ( $\text{LO}_1$ ) and a “GaAs-like” mode ( $\text{LO}_2$ ). For the alloys both  $\text{LO}_1$  and  $\text{LO}_2$  have an asymmetrical line shape ( $\Gamma_a > \Gamma_b$ ) that is broader than GaAs. We have subtracted a small background on the low-frequency side of  $\text{LO}_1$  and  $\text{LO}_2$  for the alloys due to disorder-activated zone-edge  $\text{TO}_1$  and  $\text{TO}_2$  modes. As the Al concentration increases, the  $\text{LO}_2$  mode becomes broader and more asymmetric while the reverse is true for  $\text{LO}_1$ .<sup>8,9</sup> For Al-rich samples ( $x \geq 0.8$ ) the “GaAs-like” mode line shape was complicated by the presence of the Al feature.<sup>7</sup> In Fig. 2 Raman spectrum from a typical sample of  $\text{Ga}_{0.47}\text{In}_{0.53}\text{As}/\text{InP}$  is displayed. The strong peak at  $270 \text{ cm}^{-1}$  is the “GaAs-like” LO mode. We did not detect the “InAs-like” LO feature.<sup>10,11</sup>

In an “ideal” crystal (i.e., one with translational symmetry) the spatial correlation function of the

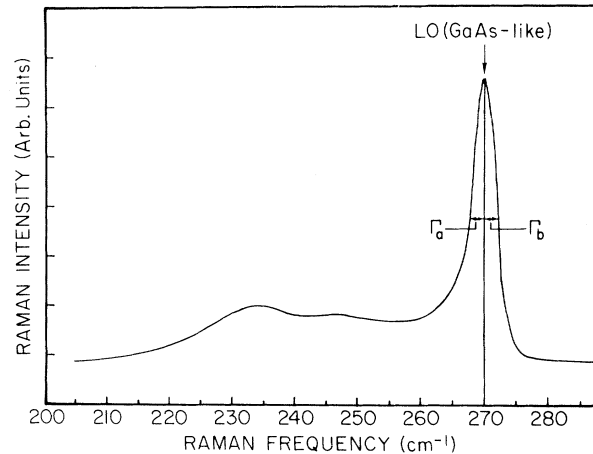


FIG. 2. Raman spectra from a representative sample of  $\langle 100 \rangle \text{In}_{0.47}\text{Ga}_{0.53}\text{As}/\text{InP}$  (sample No. 13) at 300 K.

phonon is infinite in extent and hence the phonon eigenstates are plane waves. This leads to the usual  $\vec{q} = 0$  momentum selection rules of Raman scattering. However, alloying introduces APF, and hence the mode correlations become finite,<sup>12</sup> giving rise to a relaxation of the  $\vec{q} = 0$  selection rule. A Gaussian spatial correlation function  $\exp(-2r^2/L^2)$  has been successfully used to account for  $q$ -vector relaxation related to finite-size effects<sup>13</sup> and structural disorder (ion-damaged materials)<sup>14</sup> and hence, we use it as an *Ansatz*. The Raman intensity,  $I(\omega)$ , at a frequency  $\omega$ , can then be written as

$$I(\omega) \propto \int_0^1 \exp\left\{-\frac{q^2 L^2}{4}\right\} \times \frac{d^3 q}{[\omega - \omega(q)]^2 + (\Gamma_0/2)^2}, \quad (1)$$

where  $q$  is expressed in units of  $2\pi/a$ ,  $a$  is the lattice constant, and  $\Gamma_0$  ( $= 3.0 \text{ cm}^{-1}$ ) is the width (full width at half maximum) of the intrinsic Raman line shape of the end-point materials.<sup>15</sup> For the dispersion  $\omega(q)$  of the LO phonon we take the analytical model relationship based on a one-dimensional linear-chain model<sup>16</sup>:

$$\omega^2(q) = A + \{A^2 - B[1 - \cos(\pi q)]\}^{1/2}, \quad (2)$$

where in Eq. (2)  $A = 4.26 \times 10^4 \text{ cm}^{-2}$  and  $B = 7.11 \times 10^8 \text{ cm}^{-4}$  for GaAs<sup>17</sup> and  $A = 8.20 \times 10^4 \text{ cm}^{-2}$  and  $B = 2.23 \times 10^9 \text{ cm}^{-4}$  for AlAs.<sup>8</sup> For simplicity we assume a spherical correlation region and Brillouin zone (BZ).

In Fig. 1, for the  $x=0.5$  spectrum, the dashed lines are the theoretical line shapes generated from Eqs. (1) and (2) with use of correlation lengths of

62 and 80 Å for the LO<sub>2</sub> and LO<sub>1</sub>, respectively, and the relevant dispersion relations.

Plotted in Fig. 3 are broadening  $\Gamma$  and asymmetry  $\Gamma_a/\Gamma_b$  as a function of the coherence length  $L$  as determined from Eqs. (1) and (2). The relationships calculated with the dispersion curves for AlAs and GaAs are shown by dashed and solid lines, respectively. The corresponding correlation lengths are shown on the axes marked  $L_1$  and  $L_2$ , respectively. Also plotted are the experimental points for the GaAs-like and AlAs-like modes of a number of different samples of Ga<sub>1-x</sub>Al<sub>x</sub>As/GaAs as well as the GaAs-like mode of the various Ga<sub>0.47</sub>In<sub>0.53</sub>As/InP samples. For sample No. 1 the LO<sub>1</sub> feature was too weak to extract any meaningful data. Because of the presence of the Al feature in samples No. 7, 8, and 9, we were not able to determine the linewidth and asymmetry of the LO<sub>2</sub> feature. Also, we have taken from Ref. 3 a representative experi-

mental data point, i.e., sample No. 5 (LO<sub>2</sub> mode). Representative errors in the determination of  $\Gamma$  and  $\Gamma_a/\Gamma_b$  are shown by vertical and horizontal bars, respectively, for the data of sample No. 3. The agreement between theory and the experimental points is quite good over the entire range of  $\Gamma$  and  $\Gamma_a/\Gamma_b$ .

From Fig. 3 we note that in a given crystal of GaAlAs, the GaAs-like mode may have a different spatial correlation length from that of the AlAs-like mode. In general, as the crystal becomes Al rich,  $L_1$  increases while  $L_2$  decreases. The fact that we find a linewidth  $\Gamma = 3.2 \text{ cm}^{-1}$  for sample No. 9 ( $x = 0.9$ ) indicates that the linewidth of LO phonon in AlAs is also close to that of GaAs, i.e.,  $3.0 \text{ cm}^{-1}$ . The GaInAs samples present an interesting case since they all have the same nominal composition but were prepared with different growth parameters. Figure 3 shows that there are somewhat different correlation lengths for these samples, depending not only on the growth technique, but apparently on the difference in the growth conditions for the same method. For example, samples Nos. 13 and 14, both prepared by molecular-beam epitaxy have different correlation lengths. Note that sample No. 13 has a long correlation length in relation to comparable Ga<sub>0.5</sub>Al<sub>0.5</sub>As material. Thus, these results indicate that the microscopic alloy disorder depends, in general, on the growth parameters as well as the alloy composition.

It has been suggested that the spatial correlation function should be of the form  $\exp(-r/L)$ .<sup>12</sup> The dotted line in Fig. 3 shows the relationship between  $\Gamma$  and  $\Gamma_a/\Gamma_b$  calculated by use of the appropriate Fourier transform of this function in Eq. (1) and the dispersion curve for GaAs in Eq. (2), with corresponding lengths denoted by  $L'_2$ . From Fig. 3 it is clear that these correlation functions are not suitable to describe the experimental results.

The model of Ref. 3 differs from ours in several important features: (a) A Lorentzian function was used to describe the  $q$ -vector distribution; (b) the integral is one dimensional in  $q$  space; (c) they use a quadratic frequency dispersion which is not valid over the entire BZ; and (d) to fit their data, a composition-dependent intrinsic linewidth  $\Gamma_0(x)$  had to be employed. Note from Fig. 3 that it is possible to fit the experimental data of Ref. 3 (sample No. 5) by our approach. Also, Ref. 3 fitted the asymmetry of only the GaAs-like mode and only  $x = 0.5$ . Thus the spatial-correlation model used here is much more general and the results are more comprehensive than those of Ref. 3.

While it is clear that the finite extent of a phonon

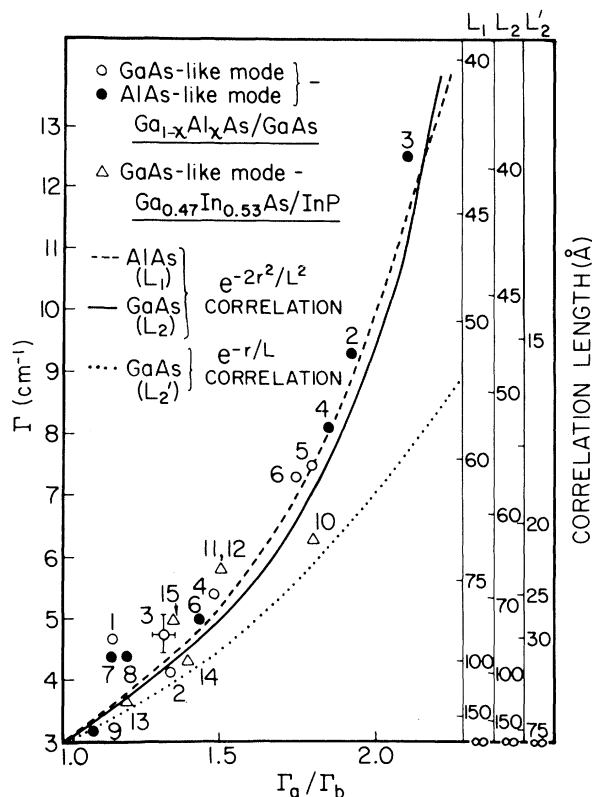


FIG. 3. The relationship between broadening  $\Gamma$  and asymmetry  $\Gamma_a/\Gamma_b$  as a function of correlation length  $L$ . The dashed line and solid line are calculated for AlAs dispersion ( $L_1$ ) and GaAs dispersion ( $L_2$ ), respectively, with use of  $\exp(-2r^2/L^2)$  as the correlation function. The dotted line shows the relationship for GaAs dispersion ( $L'_2$ ) using  $\exp(-r/L)$  spatial correlation. The experimental points for the various samples are also shown.

wave function, i.e.,  $q$ -vector relaxation, can be extended to microstructural geometries such as sublattice disorder that are not microcrystalline, it was not evident that the same spatial-correlation model should be applicable in these cases. Thus, this work combined with Refs. 13 and 14 shows that the spatial-correlation model of Eq. (1) is more general than the initial application implies and therefore indicates that it results from a rather fundamental property of the effects of the disruptions of translational symmetry on phonon propagation. It should also be mentioned that while the spatial correlation length has clear meaning for microcrystalline effects, i.e., microcrystallite size, and structural damage, i.e., average size of undamaged region, its interpretation for compositional disorder is less evident. It is probably a measure of the extent to which the sublattice is ordered, since the disruption in the periodicity is the cause for the finite spatial correlation of the phonon wave function. This conclusion is further evidenced by the composition dependence of  $L_1$  and  $L_2$  for the  $\text{Ga}_{1-x}\text{Al}_x\text{As}$  system. Thus it is clear that the parameter yields valuable information about the distribution of constituent atoms in a nominally disordered alloy.

In conclusion, we have demonstrated that the spatial-correlation model with a single physically meaningful parameter successfully accounts for the asymmetric broadening of the LO-phonon Raman line shapes induced by APF.

We would like to express our special gratitude to Dr. Nick Bottka of U. S. Naval Research Laboratories, Dr. Tom Pearsall of Bell Laboratories, Dr. Gary Wicks of Cornell University, and Dr. Jerry Woodall of IBM for providing us the samples used in this study. We gratefully acknowledge the support of this project by the IBM Shared University

Research Program.

<sup>1</sup>A. S. Barker and A. J. Sievers, *Rev. Mod. Phys.* **47**, Suppl. No. 2, 1 (1975), and references therein.

<sup>2</sup>See, for example, R. Tsu, *Proc. Soc. Photo-Opt. Instrum. Eng.* **276**, 78 (1981), and references therein.

<sup>3</sup>B. Jusserand and J. Sapriel, *Phys. Rev. B* **24**, 7194 (1981).

<sup>4</sup>T. N. Krabach, N. Wada, M. V. Klein, K. C. Cadien, and J. E. Green, *Solid State Commun.* **45**, 895 (1983).

<sup>5</sup>B. A. Weinstein, *Solid State Commun.* **20**, 999 (1976).

<sup>6</sup>P. Parayanthal, F. H. Pollak, and J. M. Woodall, *Appl. Phys. Lett.* **40**, 961 (1982).

<sup>7</sup>R. Tsu, H. Kawamura, and L. Esaki, in *Proceedings of the Eleventh International Conference on the Physics of Semiconductors, Warsaw, 1972*, edited by M. Miasek (PWN Polish Scientific, Warsaw, 1972), p. 1135.

<sup>8</sup>A. S. Barker, Jr., J. L. Merz, and A. C. Gossard, *Phys. Rev. B* **17**, 3181 (1978).

<sup>9</sup>R. Bonneville, *Phys. Rev. B* **24**, 1987 (1981).

<sup>10</sup>T. P. Pearsall, R. Carles, and J. C. Portal, *Appl. Phys. Lett.* **42**, 436 (1983).

<sup>11</sup>K. Katimoto and T. Katoda, *Appl. Phys. Lett.* **40**, 826 (1982).

<sup>12</sup>R. Shuker and R. W. Gammon, *Phys. Rev. Lett.* **25**, 222 (1970), and in *Proceedings of the Second International Conference on Light Scattering in Solids, Paris, 1971*, edited by M. Balkanski (Flammarion, Paris, 1971), p. 334.

<sup>13</sup>H. Richter, Z. P. Wang, and L. Ley, *Solid State Commun.* **39**, 625 (1981).

<sup>14</sup>K. K. Tiong, P. M. Amirtharaj, F. H. Pollak, and D. E. Aspnes, *Appl. Phys. Lett.* **44**, 122 (1984).

<sup>15</sup>M. Teicher, R. Beserman, M. V. Klein, and H. Morokoc, to be published.

<sup>16</sup>C. Kittel, *Introduction to Solid State Physics* (Wiley, New York, 1967), 3rd ed., Chap. 5.

<sup>17</sup>J. T. Waugh and G. Dolling, *Phys. Rev.* **132**, 2410 (1963).